Vazquez, A.; Rodriguez, M.; Castro-Carranza, A.; Martinez-Castillo, J.; Maldonado, J. L.; Gutowski, J.; Nolasco, J. C.:

Numerical simulation of a bilayer organic solar cell based on boron chromophore compounds as acceptors

Conference paper as: peer-reviewed accepted version (Postprint)

DOI of this document*(secondary publication): https://doi.org/10.26092/elib/3690

Publication date of this document: 17/02/2025

* for better findability or for reliable citation

Recommended Citation (primary publication/Version of Record) incl. DOI:

A. Vázquez et al., "Numerical simulation of a bilayer organic solar cell based on boron chromophore compounds as acceptors," 2020 IEEE International Conference on Engineering Veracruz (ICEV), Boca del Rio, Mexico, 2020, pp. 1-5, doi: 10.1109/ICEV50249.2020.9289666.

Numerical simulation of a bilayer organic solar cell based on boron chromophore compounds as acceptors

A. Vázquez [a], M. Rodriguez [b], A. Castro-Carranza [c,d], J. Martínez-Castillo [a], J.L. Maldonado [b], J. Gutowski [c,e] and J.C. Nolasco [a*]

[a] *Micro and Nanotechnology Research Centre MICRONA, Veracruz University, 94294, Veracruz, Mexico*

[b] *Research Group of Optical Properties of Materials (GPOM), Centro de Investigaciones en Óptica A.C., A.P. 1-948, 37000 León, Guanajuato, Mexico*

[c] *Semiconductor Optics, Institute of Solid State Physics University of Bremen, 28359 Bremen, Germany*

[d] *Laboratory of Environmental Electron Devices, Sustainable Materials, National School of Higher Studies Unit Morelia, National Autonomous University of Mexico (ENES Morelia UNAM), 58190, Morelia, Mexico*

[e] *MAPEX Center of Materials and Processes, University of Bremen, 28359 Bremen, Germany*

[*]Corresponding author: *janolasco@uv.mx*

Abstract—Organic solar cells fabricated with non-fullerene acceptors have proven to be a solution to reduce manufacturing costs. Besides the material selection, another way to reduce such costs is by optimizing the properties of both the materials and the interfaces which in turn would contribute to enhance the solar cells efficiency. This can be done with numerical simulations. Among non-fullerene materials, boron chromophores are relatively stable and chemically versatile compounds which have been usually used as donors in solar cells. In this work, planar solar cells based on PTB7 and boron compounds are proposed and simulated but by using the latter as acceptors. Specifically, we show the functionality of our proposed devices by analyzing the variation of both the Lowest Unoccupied Molecular Orbital (LUMO) and the influence of the non-intentional doping of the boron compounds with regard to the photovoltaic parameters of the solar cells. The properties of the materials such as the dielectric constant, energy levels, and non-intentional doping are taken from literature. We show that there are optimal values for LUMO and doping concentration to maximize the device efficiency. The causes of this behavior are analyzed using band diagram simulations.

Keywords— simulation, boron chromophores, LUMO, non-intentional doping

I. INTRODUCTION

Solar cells made of silicon-based semiconductors have led the global market; however, these devices need a complex manufacturing process that requires high temperatures [1]. In addition, the high amount of energy used during this process implies an increase of the costs and the generation of thermal pollution. Therefore, an alternative is the manufacturing of solar cells based on solution-processable materials.

One promising way is the fabrication of solar cells based on organic materials which feature lower manufacturing cost [1], further, their reported efficiency is still increasing up to date [2]. One of the main challenges to improve power conversion efficiency (PCE), which depends on photovoltaic parameters, i.e. fill factor (FF), density current (J_{sc}), and open circuit voltage (V_{OC}), has been to study the electron-hole pair recombination. It results in electrical losses and is a function of the semiconductor electrical properties and the solar cell interfaces.

Due to their easy synthesis and low manufacturing costs, boron composite semiconductors have been applied in solar cells [3], [4]. An additional positive characteristic of boron compounds is their tunable and high absorption. Previously, we showed the functionality of borinates as donors in a flat-band heterojunction organic cell using a small fullerene molecule (PCBM) as acceptor [5]. However, due to environmental reasons and their high costs, it is necessary to avoid the use of the fullerenes. Therefore, we study the possibility of replacing fullerene for our previously proposed organic solar cell structure. Hence, we carry out numerical simulations of solar cells based on PTB7 (poly [[4, 8 - bis [(2-Ethylhexyl) oxy] benzo [1, 2-b: 4, 5-b '] dithiophene - 2, 6- diyl] [3 - fluoro - 2 - [(2 - Ethylhexyl) carbonyl] thieno [3,4-b] thiophenediyl]]) and borinates to test their theoretical functionality and to analyze the effect of varying the borinates' properties on the solar cell performance. The simulations were carried out using the Afors-Het (**A**utomat **for s**imulation of **het**erostructure) software. This numerical simulator solves Poisson, transport, and continuity equations for electrons and holes in uniformly illuminated solar cells [6].

II. Numerical Simulation in Afors-Het

A. Device simulation parameters

Afors-Het is used to calculate energy band diagrams and J-V illuminated curves by solving Poisson's and continuity equations, respectively. The active solar cell junction is composed of two layers: (i) the donor layer, i.e. PTB7; and (ii) the acceptor layer, i.e. the borinate. Table 1 shows the physical and technological parameters of such layers, where X, E_g, $E_{g\ opt}$, and ε_r are electron affinity, bandgap energy, optical bandgap energy, and relative permittivity, respectively. The hole and electron mobilities are μ_p and μ_n. N_D and N_A are donor and acceptor non-intentional doping densities [7]. N_V and N_C are the effective valence and conduction band electronic state densities. A value of zero is assumed for N_D since most of the organic semiconductors have resulted to be non-intentionally p-type doped materials [8], [9]. Fig. 1 shows the absorption coefficient spectra of both PTB7 and a borinate as being used for the simulations. The wavelength ranges of those absorption coefficients fit well to the sun spectrum yielding a high absorption of sun photons. Other parameters taken from literature are the materials' energy levels; the graphic inset shows the LUMO and the HOMO (Highest Occupied Molecular Orbital). The energy levels must promote the separation of photogenerated excitons resulting in the transport of electrons through the borinate and the holes through the PTB7 towards their respective electrodes. The charge carrier collection also depends on the band bending which can be controlled by varying the properties of the materials [10]–[12]. This study is focused on investigating the effect of LUMO variation (from 3.18 eV to 3.58 eV) and the borinate acceptor dopant concentration (from $1x10^{10}$ to $1x10^{17}$ cm^{-3}) in the PTB7/borinate solar cells. The simulated devices correspond to ideal junctions conformed by semiconductors and interfaces without any defects.

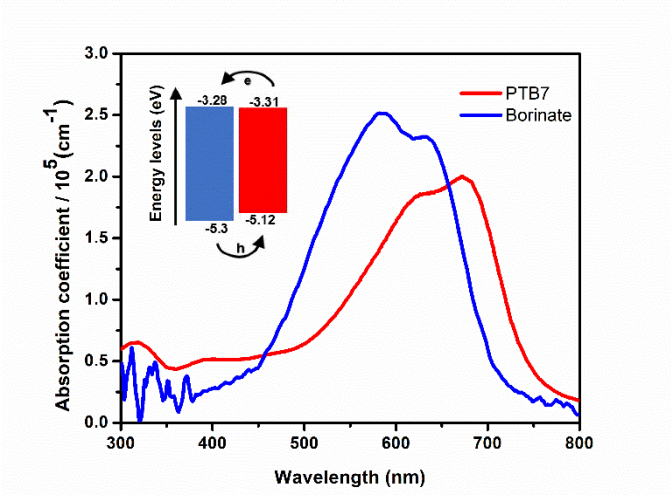

Fig. 1. Absorption spectra of PTB7 (red) and borinate (blue). Inset: Energy levels of LUMO and HOMO.

B. Optical and electrical calculations fundamentals

To understand the main working principles of Afors-Het, optical and electrical calculations should be assessed. On the one hand, to carry out the optical analysis, the Lambert-Beer absorption model is used to calculate the above-bandgap electron/hole generation. The generation rate for the above-bandgap eh pairs is related to photons with an energy of $E_{photon} = hc/\lambda \geq E_g$ with λ the photon wavelength and E_g the bandgap of the semiconductor layer that absorbs photons. The above-bandgap charge generation rate is calculated by using eq. (1). The result yields the hole and electron generation rate through the solar cells. λ_{max} and λ_{min} are provided by the spectral range of the photon flux, $\Phi(\lambda,t)$. R and A are the material reflectance and absorptance profiles of the illuminated contact. x is the position within the semiconductor layers thickness, γ is the light incidence angle on the active layer, and α is the absorption coefficient.

$$G(x,t) = \int_{\lambda_{min}}^{\lambda_{max}} d\lambda\ \Phi_0(\lambda,t)\ R(\lambda)\ A(\lambda)\ \alpha_x(\lambda) e^{\frac{-\alpha_x(\lambda)\,x}{\cos(\gamma)}} \quad (1)$$

On the other hand, the electrical phenomena at each heterojunction and contact surface can be described by different physical transport and recombination models. To perform the electrical calculations under electrostatic conditions and thus the band diagrams, it is necessary to apply Poisson's equation (2), with $\varphi(x,t)$ the electric potential, $p(x,t)$ the hole , and $n(x,t)$ the electron density,

$$\frac{\varepsilon_0 \varepsilon_r(x)}{q} \frac{\partial^2 \varphi(x,t)}{\partial x^2} = p(x,t) - n(x,t) + N_D(x) - N_A(x) \quad (2)$$

In the continuity and transport equations given by (3,4,5,6), the gradients of the corresponding quasi Fermi energy levels for electrons and holes (E_{Fn} and E_{Fp}) can drive the electron and hole currents $j_n(x,t)$ and $j_p(x,t)$, respectively.

$$-\frac{1}{q}\frac{\partial j_n(x,t)}{x} = G_n(x,t) - R_n(x,t) - \frac{\partial}{\partial t} n(x,t) \quad (3)$$

$$j_n(x,t) = q\ \mu_n\ n(x,t) - \frac{\partial E_{Fn}(x,t)}{\partial x} \quad (4)$$

$$+\frac{1}{q}\frac{\partial j_p(x,t)}{x} = G_p(x,t) - R_p(x,t) - \frac{\partial}{\partial t} p(x,t) \quad (5)$$

$$j_p(x,t) = q\ \mu_p\ p(x,t) - \frac{\partial E_{Fp}(x,t)}{\partial x} \quad (6)$$

General principles and all implemented models are detailed in [15].

TABLE 1. PHYSICAL PARAMETERS USED FOR SIMULATION.

Semiconductors	*Thickness (nm)*	*Er (-)*	*X (eV)*	*E_g (eV)*	*$E_{g\ opt}$ (eV)*	*N_C (cm^{-3})*	*N_V (cm^{-3})*	*μ_n (cm^2/Vs)*	*μ_p (cm^2/Vs)*	*N_a (cm^{-3})*	*Ref.*
PTB7	*50*	*2.27*	*3.31*	*1.81*	*1.81*	*$2.5x10^{19}$*	*$2.5x10^{19}$*	*$1x10^{-3}$*	*$1x10^{-3}$*	*$5.23x10^{16}$*	[13], [14]
Borinate	*50*	*2*	*3.28*	*1.72*	*1.66*	*$2.5x10^{19}$*	*$2.5x10^{19}$*	*$1x10^{-3}$*	*$1x10^{-3}$*	*$1x10^{10}$*	[5]

III. Results and Discussion

Fig. 2 shows simulated band diagrams of PTB7/Borinate solar cells for five borinate LUMO levels (3.18 eV, 3.28 eV, 3.38 eV, 3,48 eV, and 3.58 eV). Two relevant effects due to the LUMO variation can be pointed out from the diagrams. First, as the LUMO increases, the barriers at the heterojunction benefit charge carrier extraction. It is the potential barriers defined by the band's discontinuity promote e electrons through the borinate and the holes through the PTB7. Second, low LUMO values cause a higher band bending effect which can facilitate the drift of the charge carriers towards their respective electrode.

In Fig. 3 the J-V solar cell characteristics under illumination is depicted for the five different LUMO energies. The PCE of the corresponding devices is shown as inset in the figure. To analyze the charge collection effects, we consider the same absorption coefficients as presented in Fig. 1 for all LUMO levels. This means the same charge carrier generation rate is valid for all cases. The J-V characteristics demonstrate the functionality of our proposed solar cell structures using the borinates as acceptors in bilayer solar cells, which is the main novelty of this study. Further, the calculated efficiencies shown in Fig. 3 are similar and in some cases (3.28 eV, 3.38 eV, and 3,48 eV) even significantly higher than that obtained in our previous experimental results reaching just ~1% improvement when using fullerenes as acceptors [4]. Bulk heterojunctions solar cells based on boron compounds have reached similar efficiencies to the ones reported in this study [16]–[18].

It can be noticed that the highest efficiency is reached with a LUMO of 3.28 eV and 3.38 eV (see inset of Fig. 3). This is mainly attributed to a high J_{sc}. These results and the band diagrams in Fig. 2 indicate that the effect of a large band bending in the devices causes an increment of the extraction rate of the photogenerated charges due to the drift of the-

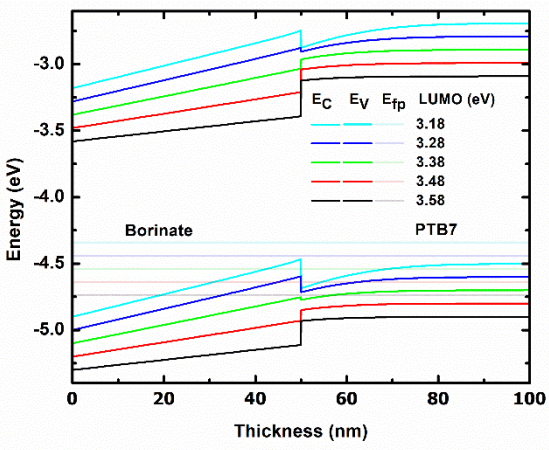

Fig. 2. Simulated band diagrams of PTB7/Borinate solar cells at different LUMO levels.

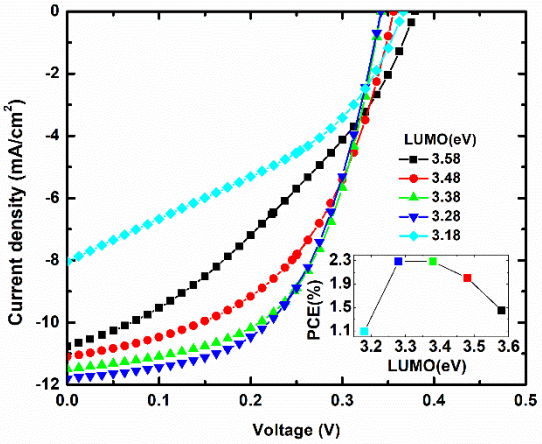

Fig. 3. Simulated current density under illuminated of PTB7/borinate solar cells at different LUMO levels. Inset: PCE at difference LUMO levels.

carriers. This phenomenon obviously dominates over the whole heterojunction, contributing even more than the presence of a potential barrier defined by the band discontinuity at the interface. When a noticeably high barrier is formed at the heterojunction (e. g., for a LUMO value of 3.58 eV, black line in Fig. 2) but being accompanied by a small band bending (flat band conditions), charge extraction becomes less favorable. The band bending effects in organic semiconductors being reported in [9] strongly support the present findings.

Fig. 4 shows simulated band diagrams of PTB7/borinate solar cells for different borinate acceptor doping levels from $1x10^{10}$ to $1x10^{17}$ cm^{-3} which is a realistic practical doping concentration range. The same HOMO level of 3.28 eV was considered for all the cases. As can be seen in Fig. 4, a rising acceptor dopant concentration causes a trend of the band bending in the device towards flat band conditions.

Again, the J-V solar cells characteristics under illumination are depicted in Fig. 5 for each mentioned doping level. The corresponding cell efficiencies are given in the inset. A clear trend towards increasing values of all photovoltaic parameters can be observed as the dopant concentration decreases, which in turn causes an increment in the efficiency of the devices. A doping concentration as low as $1x10^{10}$ cm^{-3} is the value for which the highest efficiency is reached. These results and the band diagrams in Fig. 4 indicate that band bending strongly influences the charge carrier extraction. Specifically, it is inferred that as the band bending decreases, the charge carrier extraction decreases as well, which in turn increases the recombination probability at the interface, yielding a decrease of the efficiency in these solar cells. An additional strategy for a further device-efficiency improvement could be the inclusion of a third semiconductor compound to increase photon collection and to avoid recombination.

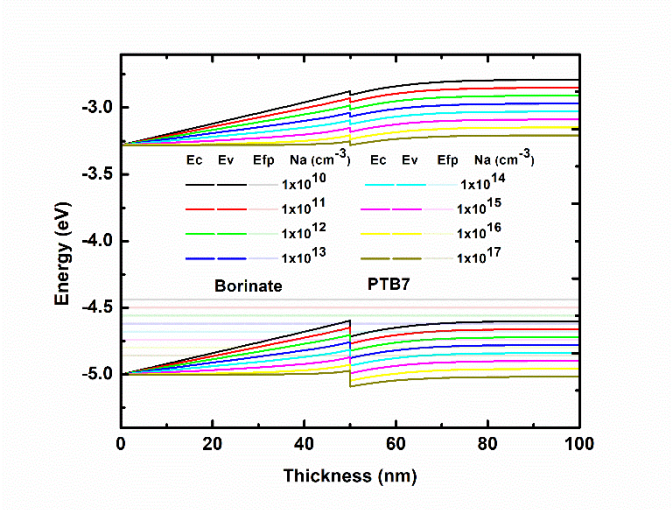

Fig. 4. Simulated band diagrams of PTB7/Borinate solar cells at different acceptor doping.

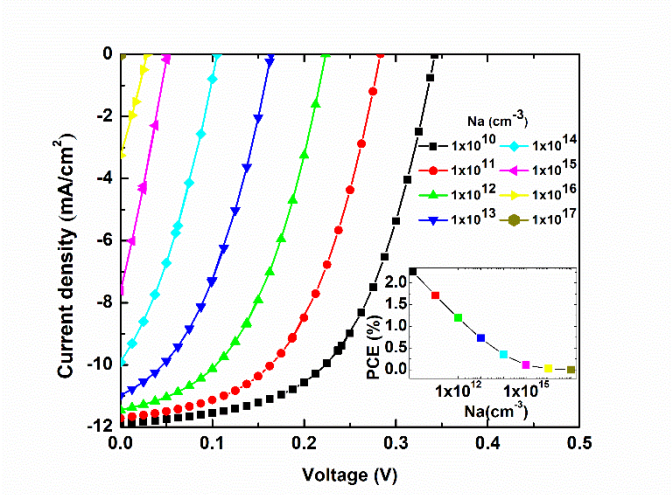

Fig. 5. Simulated current density under illuminated of PTB7/borinate solar cells at different acceptor doping. Inset: PCE at difference acceptors doping

IV. Conclusion

In this study, we carried out numerical simulations of a novel bilayer organic solar cell structure (PTB7/borinate) based on boron chromophore compounds as acceptors. We demonstrate the functionality of these solar cells. On this basis, after the variation of the acceptor material, we found that the best solar cell efficiency achieved of 2.28%, corresponds to a LUMO level of 3.28 eV and a doping concentration of $1x10^{10}$ cm^{-3}. These results and the simulated band diagrams indicate that the cause of these phenomena is mainly determined by the band bending effect, which will lead to an enhanced charge carrier extraction and collection.

Acknowledgment

A. Vazquez would like to thank CONACYT for the scholarship that supports him to develop this work. A. Castro-Carranza, J. Gutowski, and J.C. Nolasco acknowledge UNAM PAPIME project PE112720. This work has been performed in the framework of the Bremen-Mexican Network on Sustainable Technologies for Environmental Applications (BreMex-STEAps).

References

[1] M. Bhaskaran, S. Sriram, and K. Iniewski, Eds., *Energy Harvesting with Functional Materials and Microsystems*, CRC Press. Boca Raton, 2014.

[2] "Best Research-Cell Efficiency Chart | Photovoltaic Research | NREL." [Online]. Available: https://www.nrel.gov/pv/cell-efficiency.html. [Accessed: 21-Aug-2020].

[3] J.-F. Salinas *et al.*, "On the use of Woods metal for fabricating and testing polymeric organic solar cells: An easy and fast method," *Sol. Energy Mater. Sol. Cells*, vol. 95, no. 2, pp. 595–601, Feb. 2011, doi: 10.1016/j.solmat.2010.09.024.

[4] Z. El Jouad *et al.*, "The effect of the band structure on the Voc value of ternary planar heterojunction organic solar cells based on pentacene, boron subphthalocyanine chloride and different electron acceptors," *J. Phys. Chem. Solids*, vol. 136, no. August 2019, p. 109142, 2020, doi: 10.1016/j.jpcs.2019.109142.

[5] J. C. Nolasco *et al.*, "Organoboron donor-π-acceptor chromophores for small-molecule organic solar cells," *J. Mater. Sci. Mater. Electron.*, vol. 29, no. 19, pp. 16410–16415, Oct. 2018, doi: 10.1007/s10854-018-9732-6.

[6] R. Varache, C. Leendertz, M. E. Gueunier-Farret, J. Haschke, D. Muñoz, and L. Korte, "Investigation of selective junctions using a newly developed tunnel current model for solar cell applications," *Sol. Energy Mater. Sol. Cells*, vol. 141, pp. 14–23, 2015, doi: 10.1016/j.solmat.2015.05.014.

[7] B. A. Gregg, "Charged defects in soft semiconductors and their influence on organic photovoltaics," *Soft Matter*, vol. 5, no. 16, p. 2985, 2009, doi: 10.1039/b905722f.

[8] A. Guerrero *et al.*, "Interplay between fullerene surface coverage and contact selectivity of cathode interfaces in organic solar cells," *ACS Nano*, vol. 7, no. 5, pp. 4637–4646, 2013, doi: 10.1021/nn4014593.

[9] J. A. Carr and S. Chaudhary, "The identification, characterization and mitigation of defect states in organic photovoltaic devices: A review and outlook," *Energy and Environmental Science*, vol. 6, no. 12. The Royal Society of Chemistry, pp. 3414–3438, 14-Dec-2013, doi: 10.1039/c3ee41860j.

[10] J. C. Nolasco *et al.*, "Understanding the open circuit voltage in organic solar cells on the basis of a donor-acceptor abrupt (p-n++) heterojunction," *Sol. Energy*,

vol. 184, no. April, pp. 610–619, May 2019, doi: 10.1016/j.solener.2019.04.031.

[11] S. Izawa, N. Shintaku, and M. Hiramoto, “Effect of Band Bending and Energy Level Alignment at the Donor/Acceptor Interface on Open-Circuit Voltage in Organic Solar Cells,” *J. Phys. Chem. Lett.*, vol. 9, no. 11, pp. 2914–2918, Jun. 2018, doi: 10.1021/acs.jpclett.8b01134.

[12] N. Shintaku, M. Hiramoto, and S. Izawa, “Doping for Controlling Open-Circuit Voltage in Organic Solar Cells,” *J. Phys. Chem. C*, vol. 122, no. 10, pp. 5248–5253, Mar. 2018, doi: 10.1021/acs.jpcc.7b12203.

[13] N. Gasparini *et al.*, “Designing ternary blend bulk heterojunction solar cells with reduced carrier recombination and a fill factor of 77%,” *Nat. Energy*, vol. 1, no. 9, p. 16118, Sep. 2016, doi: 10.1038/nenergy.2016.118.

[14] B. Ebenhoch, S. A. J. Thomson, K. Genevičius, G. Juška, and I. D. W. Samuel, “Charge carrier mobility of the organic photovoltaic materials PTB7 and PC71BM and its influence on device performance,” *Org. Electron.*, vol. 22, pp. 62–68, 2015, doi: 10.1016/j.orgel.2015.03.013.

[15] R. Stangl, C. Leendertz, and J. Haschke, “Numerical Simulation of Solar Cells and Solar Cell Characterization Methods: the Open-Source on Demand Program AFORS-HET,” in *Solar Energy*, no. February, InTech, 2010.

[16] R. Pandey, A. A. Gunawan, K. A. Mkhoyan, and R. J. Holmes, “Efficient organic photovoltaic cells based on nanocrystalline mixtures of boron subphthalocyanine chloride and C 60,” *Adv. Funct. Mater.*, vol. 22, no. 3, pp. 617–624, 2012, doi: 10.1002/adfm.201101948.

[17] B. Kim, B. Ma, V. R. Donuru, H. Liu, and J. M. J. Fréchet, “Bodipy-backboned polymers as electron donor in bulk heterojunction solar cells,” *Chem. Commun.*, vol. 46, no. 23, pp. 4148–4150, 2010, doi: 10.1039/b927350f.

[18] M. M. Morgan *et al.*, “Boron–nitrogen substituted dihydroindeno[1,2- b]fluorene derivatives as acceptors in organic solar cells,” *Chem. Commun.*, vol. 55, no. 74, pp. 11095–11098, 2019, doi: 10.1039/C9CC05103A.